Resolved observations of geostationary satellites from the 6.5 m MMT

Michael Hart,[1,2] Richard Rast,[3] Stuart Jefferies,[2,1] Douglas Hope[4]
[1]*Steward Observatory, University of Arizona, 933 N. Cherry Ave., Tucson, AZ 85721*
[2]*Institute for Astronomy, University of Hawaii, 34 Ohia Ku Street, Pukalani, HI 96768*
[3]*AFRL/RDST, 3550 Aberdeen Ave SE, Kirtland AFB, NM 87117-5776*
[4]*US Air Force Academy, Dept. of Physics, 2354 Fairchild Dr., Colorado Springs, CO 80840*

ABSTRACT

We report observations of a number of geostationary spacecraft recorded in the *J*, *H*, and K_s bands (centered around 1.2 μm, 1.6 μm, and 2.2 μm) at the 6.5 m MMT telescope in January 2015. With adaptive optics, the satellites were resolved at close to the diffraction limit in each of the wavebands. True color images may be recovered from the multiple wavebands, while the large aperture allows accurate photometric calibration with excellent time resolution of even small, faint objects in these distant orbits. Of note are our observations of solar panels, which can only be satisfactorily imaged in bands longer than their cut-off wavelengths. Since the cut-off is generally in the neighborhood of 1.5 – 2 μm, the panels will only be well resolved by telescopes larger than 4 m. In one case observed at the MMT, solar panels were seen to span approximately 24 m, twice the extent described in published data.

1 MOTIVATION

Satellites in geostationary Earth orbit (GEO) are of particular importance for both military and civil applications, providing global communications as well as persistent monitoring for weather forecasting, missile launch detection, and other purposes. They are also particularly vulnerable since there is (at least at present) no means to service them once they are on orbit, and replacing a GEO satellite is extremely expensive and time consuming. A means to monitor the health and environs of these high-value assets from ground stations is therefore highly desirable.

Present data collection modalities for space domain awareness (SDA) are of limited value for objects in GEO. Their distance means that they are beyond the range of all but the most powerful radar systems, and although it may be possible with measurements of sufficient signal-to-noise ratio to estimate radar cross-sections, ranges, and range rates [1], the achievable lateral resolution is low because of the long wavelength of RF radiation. Even at electro-optical (EO) wavelengths, telescopes of several meters diameter, equipped with high-order adaptive optics (AO), are required before even large GEO objects will appear as anything more than unresolved blobs of light. Such information of course is valuable in determining orbits, and considerable work has been done to infer shape and attitude from light curves obtained simultaneously from multiple sites which see an object from different perspectives [2–5]. But directly resolved images at high resolution can reveal information about a satellite's orientation, configuration, and dynamical behavior that is very difficult to acquire otherwise. By way of example, as demonstrated in the work described in this paper, resolved images allow a direct assessment of the size, and therefore the power capacity, of a GEO satellite's solar panels. Knowing the power that the bus has available to it is key to inferring the satellite's capabilities.

Additional information may be derived from images with high contrast as well as high resolution. Of particular value in the context of asset protection is the ability to detect faint objects that are very close to larger, brighter spacecraft. A new generation of microsatellites – systems weighing a few tens of kilograms at most and having cross sections of a few tenths of a square meter – pose potential threats to high-value assets in GEO. Such objects have visual magnitudes no brighter than 14. While wide field space surveillance search systems such as the Space Surveillance Telescope [6] and PanSTARRS [7] are configured to find such objects there remains the significant challenge that a microsatellite in close proximity – a few hundred meters – to a large GEO satellite would be invisible to these telescopes since its signal would be swamped by the much brighter seeing disc of the large satellite.

High resolution imaging requires a large effective aperture. This is the reason for DARPA's ongoing interest in applying the principles of interferometry to GEO imaging [8,9]. However, existing large astronomical telescopes can already resolve GEO objects [10–12] provided that AO is used to overcome the degrading effects of atmospheric turbulence on both image resolution and contrast. A further advantage of large telescopes over those used for SDA today, and even compared with present long-baseline interferometers, is their light collecting power. This improves

the efficiency of an attached optical sensor in terms of its rate of production of useable intelligence, and allows high time resolution light curves to be generated from which dynamical information may be inferred that would otherwise be unavailable.

In this paper, we present data acquired with the 6.5 m MMT telescope in a joint program of the University of Arizona and the Air Force Research Laboratory. Several GEO objects were imaged in three near infrared (NIR) bands. The derived results illustrate the utility of large aperture EO/IR telescopes in addressing SDA objectives.

2 MMT OBSERVATIONS

Data for the study were acquired at the 6.5 m MMT telescope on Mt. Hopkins, AZ in January 2015. Extensive imaging of several objects in geostationary orbits was carried out in three NIR wavebands between 1.2 μm and 2.2 μm. The MMT's natural guide star adaptive optics (AO) system was used, with the GEO objects themselves serving as the reference beacons, delivering compensated imaging to the diffraction limit of the 6.5 m aperture in these wavebands.

The imaging camera was the ARizona Infrared imager and Echelle Spectrograph (ARIES), which uses a 1024×1024 NICMOS focal-plane array [13]. The image scale may be selected as 0.04 arcsec/pixel or 0.02 arcsec/pixel, yielding FOV of 40 arcsec and 20 arcsec respectively. The latter offers Nyquist sampling at all wavebands used.

The objects studied included communications satellite Anik F2 and others, as well as smaller objects and a tumbling rocket body. Data sequences were recorded in the *J*, *H*, and K_s filters with an exposure time of 1 s at a cadence of approximately one frame every 6 s, limited by the read-out time of the focal plane array. In-frame photometric calibration was carried out using the SSP package developed by HartSCI LLC, which automatically finds and identifies serendipitous star detections such as the one illustrated in Figure 1.

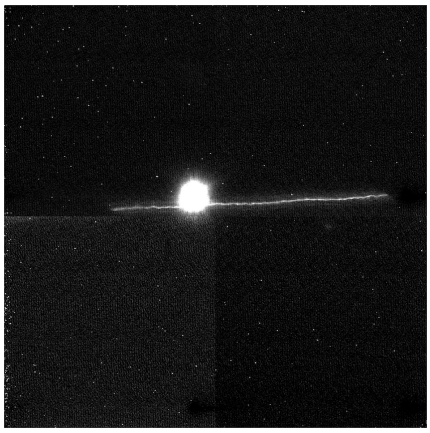

Figure 1. Representative 1 s raw exposure in *H* band of a GEO object on the ARIES camera. The gray scale shows the object saturated to highlight a star streak of the sort used for in-frame photometric calibration. The FOV is 20 arcsec.

3 ANALYSIS AND RESULTS

Telesat's Anik F2 telecommunications satellite is built around a Boeing 702 bus with solar panels spanning 48 m. It is therefore among the largest GEO spacecraft presently on orbit. Stationed at 111°W, it is also very close to the meridian as seen from the MMT. Images of the satellite were recorded in all three wavebands. A color composite image is shown in Figure 2, where the RGB channels are the K_s, *H*, and *J* bands respectively, with integration times of 64 s in each band. The final resolution is approximately 9 m, and each pixel spans 3.5 m on the satellite. Although the resolution is limited, one clearly distinguishing feature is that the solar panels, extending above and below the bus, are markedly redder than the bus itself. This is to be expected, since the panels are designed to reject wavelengths longer than about 1.8 μm which would contribute only to heating rather than power generation. They therefore appear bright in the K_s images and much fainter in the other two bands.

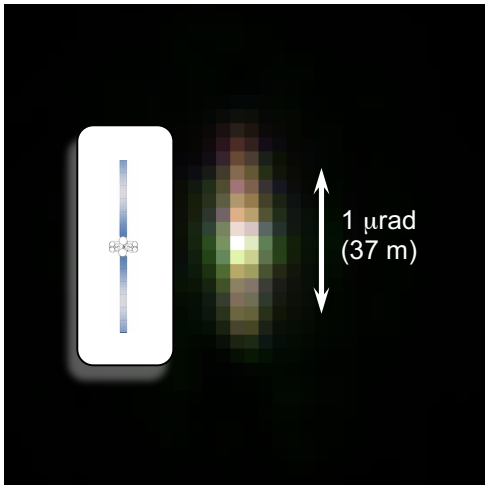

Figure 2. True-color image of Anik F2 made from separate images in *J*, *H*, and K_s bands. Note the red color of the solar panels compared to the bus. Each pixel spans 3.5 m at the satellite. A cartoon of the satellite is shown at the same scale as the image.

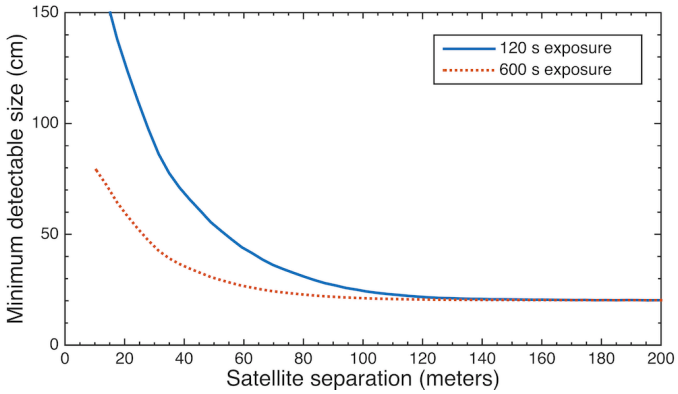

Figure 3. Quantitative detectability of microsatellites in 2 minute and 10 minute exposures at K band.

The use of AO not only improves image resolution by directing the energy back where it should go, but by moving energy away from places in the image where it should *not* be, the contrast ratio in the vicinity of an object is improved as well. This is illustrated in Figure 3 which plots the diameter of the smallest microsatellite that could be detected as a function of separation from the Anik F2 bus when imaged in the K_s band. The results are calculated assuming a faint unresolved spherical object with the same albedo as the bright satellite. The PSF is assumed to be the same for the bright and faint objects, since they are by hypothesis within the same isoplanatic patch. The results are scaled to assumed total integration times on the detector of 2 minutes and 10 minutes. The lower limit of detectable brightness is taken to be 5× the local rms noise computed from the actual Anik F2 images. The detection limit out to about 100 m separation is set by the halo of scattered light from the main satellite, which in turn is determined by the degree of correction of the AO. At larger separations, the achievable contrast is dominated by pattern noise on the detector. The detection thresholds could be improved still further through better wave-front compensation which would drive more of the light into the main satellite image, leaving less in the scattered halo, and by use of a newer generation of NIR focal-plane array than the detector in ARIES which is now nearly two decades old. Nevertheless, we have shown that at a separation of only 100 m from a bright GEO satellite, an object of just 20 cm can readily be detected in a few minutes of integration time with a 6.5 m telescope.

High temporal resolution light curves have been computed from two of our observed objects. The first, an expended Delta IV rocket body, had a mean K_s-band magnitude of about 9. Figure 4 reflects the uncontrolled tumble of the booster over 3.5 consecutive full periods spanning approximately 40 minutes of continuous observation time. With

respect to a fixed position on the ground, the rotation period is 11 m 11 s ±2 s. From one period to the next, the details of the light curve reproduce well. The strong signal at approximately 0.23 hr is not reproduced at the three other maxima; that is because of the relative phasing of the specular solar reflection, expected to last 0.9 s, from the curved booster surface and the 1 s integration time within the 6 s inter-frame period. The in-frame photometric calibration establishes the brightness of this object to about ±5%.

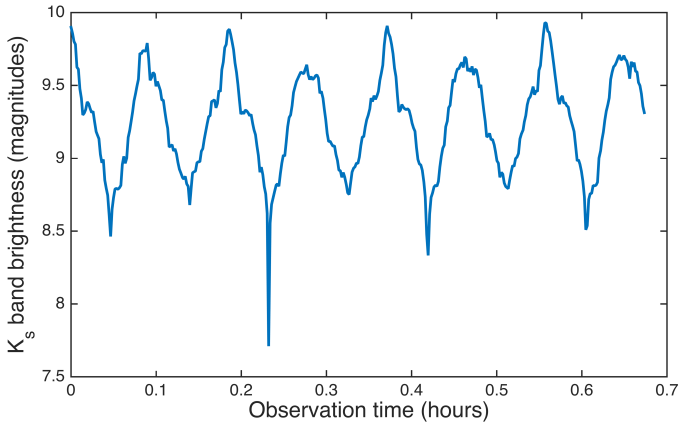

Figure 4. K_s-band light curve of a tumbling rocket body spanning 3.5 rotations.

The second object was much smaller than the rocket body, and on average approximately 4.5 magnitudes (a factor of 60) fainter. The light curve is shown in Figure 5. The curve is clearly noisier, consistent with reduced SNR. The noise is expected to be worse by the ratio of the object brightness, since it is dominated by the pattern noise of the detector rather than the photon flux of the sources. A sudden reduction in brightness of the object by a factor of about 2.5 is observed at 0.08 hr in the observing sequence. It cannot be attributed to a change in the optics or atmospheric transparency: photometric calibrator stars embedded within the observing sequence do not display the same behavior. Although we have no ground-truth information on the satellite behavior to explain the observation, the sustained brightness change is well above the noise and reflects a real change in the spacecraft's appearance.

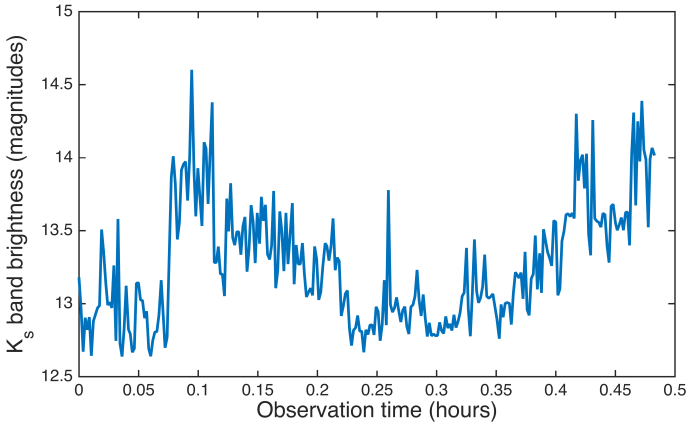

Figure 5. K_s-band light curve of a small satellite at GEO range illustrating the detection of a sudden change in solar reflection at around 0.08 hours.

An additional satellite imaged in the three bands was expected to be unresolved except at the longest wavelength, where the solar panels should be highly reflective. This was indeed the case, as illustrated in Figure 6 which shows 30 s exposures in each color after Richardson-Lucy restoration using stellar PSFs recorded in the corresponding bands at around the same time. However, surprisingly, the overall span of the spacecraft appeared to be substantially larger than published data led us to expect. Where we anticipated a marginally resolved image in the red band suggestive of a 12 m span, the K_s band image shows a clearly resolved object with an estimated length of 24 m.

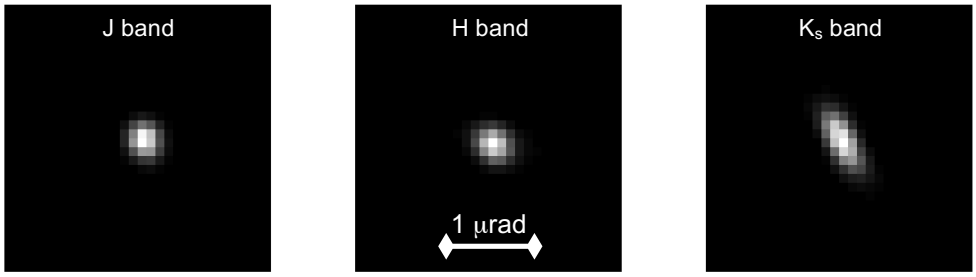

Figure 6. Images of the same GEO satellite in the three IR wavebands *J*, *H*, and K_s. Note that the solar panels are resolved only at the reddest wavelength.

We note that although the spacecraft is unambiguously resolved at 2.2 μm, the angular extent is only twice the diffraction-limited resolution element of the 6.5 m aperture at that wavelength. It is immediately clear then that the size of the panels could not be directly established with any telescope in the 3-4 m class: the panels are invisible at shorter wavelengths, below the optical stack cut-off, and diffraction by the smaller aperture would obscure the size at any wavelength long enough that the panels could be seen, either in reflection or in self emission. This is true even were the telescope in space, unless it were placed close to the object of interest.

4 CONCLUDING REMARKS

Large astronomical telescopes have a distinct role to play in situational awareness at GEO. The light grasp they offer, as well as the angular resolution and contrast when equipped with AO, enable them to deliver data products that complement those provided by existing tools and are difficult to obtain by any other means. Resolved imagery of GEO objects allows health monitoring and capability assessment; small, faint objects at close spacing may be rapidly detected and dynamically monitored. Other behavior of both spatially resolved and unresolved objects may also be dynamically tracked. Although we have not addressed the point in this paper, AO-fed spectroscopy which may be done with the ARIES instrument in the IR bands is also enabled by the large light grasp and would provide spatially-resolved information on materials content.

Large telescope facilities are expensive. General-purpose astronomical telescopes of the present generation cost on the order of $1-2M per square meter of collecting area. While it is likely that the cost for new telescopes can be greatly reduced through use of innovative light-weight materials and fabrication technologies, and by tailoring the system design to specific SDA requirements, such facilities will always represent a major investment. Astronomers, of course, will continue to make those investments, increasingly with private support, because they are essential to advancing our understanding of the Universe. Most of the present and future large-scale astronomical telescopes can in principle also contribute to SDA, serving military, civil, and commercial needs. In that sense, our use of the MMT serves as an illustration of the value of incorporating the unique data that these "non-traditional" sensors can generate into the global network of space surveillance systems.

Beyond the sensor itself, there is a need to develop the data processing and transmission pipelines to convert the data into knowledge about the space environment and to communicate that knowledge to decision makers. DARPA's StellarView and SpaceView [14] programs represent path-finding efforts to do so. They will serve as role models for the creation of larger cyberinfrastructure facilities to handle a much more substantial stream of data. As a case in point, the Large Synoptic Survey Telescope (LSST) [15] by itself will generate 30 TB of data per night, scanning the entire sky observable from its site on Cerro Pachon in Chile every 3-4 nights. Recognizing this coming need, the University of Arizona (UA) expects to stand up a processing center, using infrastructure already created by UA's iPlant collaborative [16], to analyze data streamed from the LSST, as well as other astronomical telescopes in a global network, specifically in support of SDA objectives.

5 ACKNOWLEDGEMENTS

This work has been supported by the United States Air Force Office of Scientific Research. The opinions, findings and conclusions expressed in this paper are those of the authors and do not necessarily reflect the views of the United States Air Force. Observations reported here were made with the MMT telescope, a joint facility of the

University of Arizona and the Smithsonian Institution. We are grateful to D. McCarthy and C. Kulesa for their critical assistance with the data collection, and the staff of the MMT Observatory for supporting these non-standard observations.

6 REFERENCES AND LINKS

[1] Mehrholz, D. "Radar observations of geosynchronous orbits," Second European Conference on Space Debris, Darmstadt, Germany, ESA-SP 393, 51 (1997)
[2] Fulcoly, D. O., Kalamaroff, K. I., and Chun, F. K. "Determining basic satellite shape from photometric light curves," *J. Space. Rock.*, 49, 76–82 (2012)
[3] Hall, D. et al. "AMOS Observations of NASA's IMAGE Satellite," Proc. AMOS Tech. Conf. (2006)
[4] Hall, D., Calef, B., Knox, K., Bolden M., and Kervin, P. "Separating attitude and shape effects for non-resolved objects," Proc. AMOS Tech. Conf. (2007)
[5] Hall, D. and Kervin, P. "Analysis of faint glints from stabilized GEO satellites," Proc. AMOS Tech. Conf. (2013)
[6] Monet, D. et al. "Rapid cadence collections with the Space Surveillance Telescope," Proc. AMOS Tech. Conf. (2012)
[7] Kaiser, N. et al. "Pan-STARRS: a large synoptic survey telescope array," in Survey and Other Telescope Technologies and Discoveries, eds. J. A. Tyson & S. Wolff, (Proc. SPIE) 4836, 154–164 (2002)
[8] http://www.darpa.mil/program/galileo
[9] Hart, M. et al. "Adaptive optics for fiber-fed interferometers," in Micro- and Nanotechnology Sensors, Systems, and Applications V, eds. T. George, M. S. Islam, & A. K. Dutta, (Proc. SPIE) 8725, 87250U (2013)
[10] Worden, S. P. "Observing deep-space microsatellites with the MMT and Large Binocular Telescopes," Proc. AMOS Tech. Conf. (2005)
[11] Hart, M. et al. "Wide field astronomical image compensation with multiple laser-guided adaptive optics," in Adaptive Coded Aperture Imaging, Non-Imaging, and Unconventional Imaging Sensor Systems, eds. S. Rogers, D. P. Casasent, J. J. Dolne, T. J. Karr, & V. L. Gamiz, (Proc. SPIE) 7468, 74680L (2009)
[12] Drummond, J. D. and Rast, R. H. "First resolved images of a spacecraft in geostationary orbit with the Keck-II 10 m telescope," Proc. AMOS Tech. Conf. (2010)
[13] McCarthy, D. W. et al. "ARIES: Arizona infrared imager and echelle spectrograph," in Infrared Astronomical Instrumentation, ed. A. M. Fowler, (Proc. SPIE) 3354, 750-754 (1998)
[14] Gleckler, A., Butterfield, M., Copenhaver, R., Wade, A., and Apponi, A. "SpaceView (viral Space Situational Awareness) one year update," Proc. AMOS Tech. Conf. (2013)
[15] Sweeney, D. W. "Overview of the Large Synoptic Survey Telescope project," in Ground-based and Airborne Telescopes, ed. L. M. Stepp, (Proc. SPIE), 6267, 626706 (2006)
[16] Goff, S. A. et al. "The iPlant collaborative: cyberinfrastructure for plant biology," *Front. Plant Sci.*, 2:34, 1–16 (2011)